Evidence for spin clusters and glassy behaviour in $Bi_{1-x}Ca_xMnO_3$ ($x \sim 0.875$)

2004 J. Phys.: Condens. Matter 16 2689

(http://iopscience.iop.org/0953-8984/16/15/020)

INSTITUTE OF PHYSICS PUBLISHING JOURNAL OF PHYSICS: CONDENSED MATTER

J. Phys.: Condens. Matter **16** (2004) 2689–2705 PII: S0953-8984(04)73952-1

Evidence for spin clusters and glassy behaviour in $Bi_{1-x}Ca_xMnO_3$ ($x \sim 0.875$)

Hyungje Woo[1,4], **Trevor A Tyson**[1], **Mark Croft**[2] and **Sang-Wook Cheong**[2,3]

[1] Department of Physics, New Jersey Institute of Technology, Newark, NJ 07102, USA
[2] Department of Physics, Rutgers University, Piscataway, NJ 08855, USA
[3] Bell Laboratories, Lucent Technologies, Murray Hill, NJ 07974, USA

Received 29 December 2003
Published 2 April 2004
Online at stacks.iop.org/JPhysCM/16/2689
DOI: 10.1088/0953-8984/16/15/020

Abstract

Detailed magnetic and transport properties of electron-doped $Bi_{0.125}Ca_{0.875}MnO_3$ materials are reported. Low field magnetization measurements provide evidence for ferromagnetic Curie–Weiss behaviour at higher temperatures and an antiferromagnetic state below $T_N = 109$ K, which supports a ferromagnetic component. High field ($-30\,T \leqslant H \leqslant 30\,T$) DC magnetization measurements (5–300 K) show a strongly nonlinear field response below and far above the ordering temperature. The residual magnetic moment and coercive field, in the ordered state, are, however, exceptionally small. These results are discussed in terms of the FM coupling of spins into clusters. The possible coupling of these clusters to the AF staggered magnetization (below T_N) and to AF fluctuations (above T_N) is discussed. The magnetic effects appear to be consistent with canted antiferromagnetism, however, FM segregation is not ruled out. The high field magnetoresistance (up to 30 T) appears to be governed by a field-induced reduction in the doped carrier localization. The glassy character of the cluster magnetic response was investigated by measuring the frequency dependent AC susceptibility and time/history evolution of the low field magnetization. Glassy behaviour in the cluster response is indeed observed and is discussed. The differentiation of cluster glass versus canted-AF origins of the time/history effects is still an open issue.

(Some figures in this article are in colour only in the electronic version)

1. Introduction

As a function of temperature, pressure, doping and cation radius, perovskite mixed-valent manganites show novel structural, electron transport and spin alignment transformations [1]. The phase diagram of the prototypical $La_{1-x}Ca_xMnO_3$ (LCMO) system is well characterized by extensive structural, magnetic and transport measurements [1]. For $0 < x < \sim 0.21$, the

[4] Present address: Physics Department, Brookhaven National Laboratory, Upton, NY 11973-5000, USA.

system is an insulator (I) with a canted antiferromagnetic (CAF) and ferromagnetic moment in a ground state. For the range $\sim 0.21 < x < 0.5$ a ferromagnetic (FM) metallic ground state occurs, which undergoes concomitant metal-to-insulator (MI) and FM-to-paramagnetic transformations over the temperature range 150–250 K [1h].

Compared to the $x < 0.5$ colossal magnetoresistance FM region, the $x > 0.5$ region has been less extensively studied. In the range $0.50 < x < \sim 0.875$, one finds a charge/orbital (CO) and AF ordered ground state with insulating behaviour. For x above about 0.9, the CO order disappears and the G-type AF order, observed in $CaMnO_3$, appears [2]. However, a substantial ground state FM component, originally ascribed to canted AF behaviour, appears in this high x range and peaks with significant magnitude near $x = 0.875$ [3–8]. More recently the notion of FM clusters and local phase segregation have been invoked to explain the FM response in this composition range [9–11]. A reduction in the resistivity, yielding values typical of semiconductors, accompanies the peak in the FM moment near $x = 0.875$.

Because of the enhanced moments found in this region of the phase diagram, more recent work has focused on understanding this high Ca region. Neumeier *et al* [4] suggested that electron-doped $CaMnO_3$ in $0.8 \leqslant x \leqslant 1.0$ of $La_{1-x}Ca_xMnO_3$ exhibits magnetic phase segregation with strong competition between the local FM and the long range AFM order, as compared to the standard model of CAF order in this region of the phase diagram. Troyanchuk *et al* [12] showed that the $Eu_{1-x}Ca_xMnO_3$ system also manifested a FM component in the $0.8 \leqslant x \leqslant 1.0$ range. Again, FM/AF phase coexistence was inferred, based on the observed saturation moments. Maignan *et al* [9] showed that the electron-doped manganite $Sm_{1-x}Ca_xMnO_3$ ($0 < x \leqslant 0.2$) behaves like a semimetal in the temperature range 200–300 K. In addition, based on magnetic susceptibility and magnetization measurements, they found evidence for cluster glass behaviour for $0.88 \leqslant x < 1.0$. For example, no saturation of the magnetization was found in fields as high as 5 T. A systematic study of a broad range of materials in the system $L_{1-x}A_xMnO_3$ (L = Pr, Sm; A = Ca, Sr) was performed by Martin *et al* [10]. In direct contrast with the hole-doped Mn^{3+} rich region results [13], they found that large magnetoresistance in the Mn^{4+} rich region required a small cation radius. $Sm_{1-x}Ca_xMnO_3$ (SCMO) and $Pr_{1-x}Ca_xMnO_3$ (PCMO) were observed to fall into a class of manganites which are insulators over the entire doping region while $Pr_{1-x}Sr_xMnO_3$ mimics the behaviour of the classic $La_{1-x}Ca_xMnO_3$ system. The small Ca-ion-doped systems $Sm_{1-x}Ca_xMnO_3$, $Pr_{1-x}Ca_xMnO_3$ and $La_{1-x}Ca_xMnO_3$ all show a peak in low temperature magnetization near $x \sim 0.9$. The high net moments in these systems were attributed to cluster glass formation based on AC susceptibility measurements. It should be emphasized, however, that neutron scattering measurements on the material clearly showed the presence of G-type AF order coexisting with this FM-cluster glass behaviour [12]. Interestingly even in the end-member, $CaMnO_3$, weak ferromagnetism is observed along with G-type AF order [12, 14].

In $Bi_{1-x}Ca_xMnO_3$, Bao *et al* [15] found the fact that dynamic ferromagnetic spin correlations at high temperature are switched into antiferromagnetic spin fluctuations below charge-structural transition temperature, T_O. Chiba *et al* [8] observed that the low temperature resistivity drops continuously when $CaMnO_3$ is electron-doped with Bi^{3+}, and reaches a minimum at $x = 0.875$ with magnitude characteristic of a semiconductor. At this doping, the Néel temperature approaches the paramagnetic Curie temperature (θ) and a maximum saturation magnetization of 1.1 μ_B per Mn site (compared to the theoretical saturation value of 3.1 μ_B per Mn site) is observed.

Thus, the substitution region near $x \sim 0.875$ exhibits anomalous and not yet clearly understood properties in a range of manganite systems. In particular, it is not clear if the large moment found per Mn ion is due to spin canting, spin glass or spin cluster behaviour or some more novel magnetic structure.

Extending our recent work on the $Bi_{1-x}Ca_xMnO_3$ (BCMO) system [7], we have focused the present investigation on the anomalous magnetic/transport properties near $x \sim 0.875$. Low and high magnetic fields (up to 30 T) magnetization and resistivity measurements were reported. The long-time and frequency dependence of the magnetization has been studied in detail to probe for glass-like behaviour. The combined experiments provide evidence for cluster and glass-like behaviour (in addition to AF correlations) in this $x \sim 0.875$ BCMO material (and by inference in the more general class of electron-doped manganites).

2. Experimental procedure

Polycrystalline samples of BCMO at $x = 0.875$ were synthesized by the standard solid-state reaction method. Stoichiometric mixtures of Bi_2O_3, $CaCO_3$ and MnO_2 were ground and pressed into pellets that were then calcined at 1000 °C in air for 5 h. After calcination, the samples were reground and sintered at 1200 °C in air for 5 h. This was repeated at 1250 °C. DC magnetization measurements were performed with a Quantum Design SQUID magnetometer (MPMS-XL) between 4.2 and 300 K in fields up to 50 Oe. AC susceptibility was measured by a Quantum Design MPMS (1 T model with ultra-low field options).

The high field magnetization and resistivity measurements (up to 30 T) were performed using the cell no 8 32 mm bore magnet at the National High Magnetic Field Laboratory. A vibrating sample magnetometer was used for magnetization measurements and the standard four-probe method for resistivity was employed.

3. Results

3.1. Low field magnetic response

Recent interest in hole-doped (Mn^{3+} based) manganate materials stems from their ferromagnetic and magnetoresistive properties. The occurrence of FM-like interactions has naturally broadened this field to electron-doped (Mn^{4+} based) manganates. We have chosen the $x = 0.875$ composition of the $Bi_{1-x}Ca_xMnO_3$ system for study since it represents the optimal composition with maximum magnetic moment [8]. The sharply peaked magnetization is emphasized in the inset of figure 1 where we show the magnetization (in Bohr magnetons per Mn ion at $H = 1$ T) as a function of doping. The data from this work (solid squares) are compared to the previous work of Chiba *et al* [8]. For the LCMO system, a similar maximum in the magnetization was also reported [1g, 4].

The thermal behaviour of the ferromagnetic component for this $x = 0.875$ material is illustrated in figure 1 where the temperature dependence of the low field (50 Oe) magnetization and inverse magnetic susceptibility χ^{-1} are shown. Fitting the high temperature (170–300 K) χ^{-1} behaviour to a Curie–Weiss ($[\chi = C/(T + \theta)]$) form one finds $\theta = -100$ K. Importantly this FM-θ value is quite close to (but slightly below) the AF ordering temperature $T_N = 109$ K. Below the AF ordering temperature the field-cooled (FC) magnetization (figure 1) follows a temperature dependence reminiscent of magnetic order parameter behaviour. Indeed $T_N = 109$ K has been chosen from the negative inflection point of the magnetization rise. The zero-field cooled (ZFC) magnetization has a much more complicated thermal behaviour, emphasizing the role of thermal/field history in this material which will be discussed below.

3.2. High field and small remnant magnetization

In figure 2(a) we present high field (to 30 T) hysteresis loop magnetization measurements below and above the transition temperature. The magnetization is clearly strongly nonlinear at all temperatures below 175 K. In the 5–50 K range, the magnetization appears to be made up

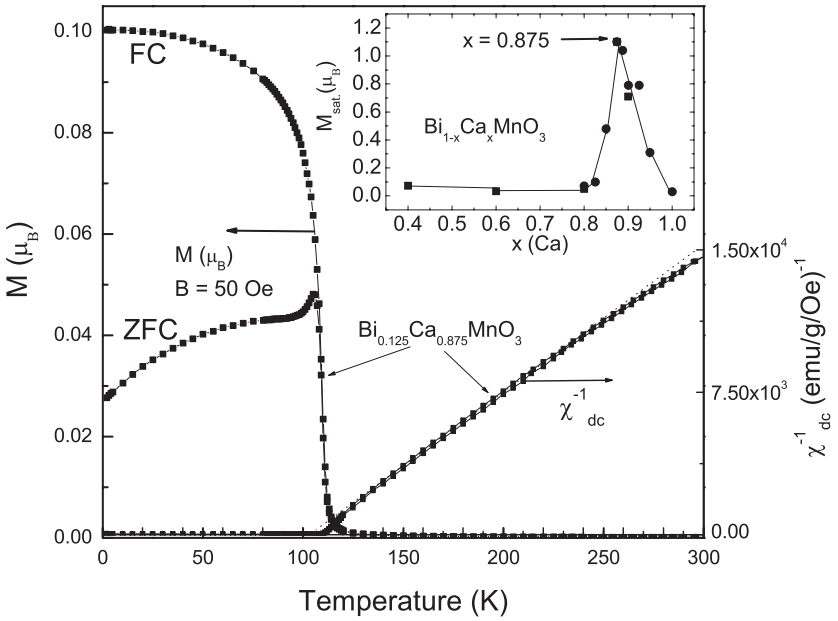

Figure 1. The magnetization curves, taken with increasing temperature, under zero-field cooled (ZFC) and field cooled (FC) conditions for $Bi_{1-x}Ca_xMnO_3$, $x = 0.875$. The FC curve shows the onset of the FM-like moment below the ordering temperature. The inverse magnetic susceptibility (χ^{-1}) versus temperature illustrates the Curie–Weiss behaviour with a FM θ (the upper curve is for cooling down and lower one is for warming up and the dotted line is a straight line). The inset shows magnetization (Bohr magneton) versus Ca doping x at 1 T. The highest moment is found at $x = 0.875$. Note that the filled squares are our data and the filled circles are from the data from Chiba *et al* [8].

of two components: a strongly nonlinear component which saturates (at about 1.25 μ_B) in the 10–15 T range, and a smaller linear component of about 0.0052 μ_B T^{-1}. Even at 30 T the full magnetization is 1.41 μ_B, far less than the theoretical limit of 3.1 μ_B. Reducing the field from 30 T to 0 yields a very small remnant (see figure 2(c)), of about 0.08 μ_B, which is suppressed by just a 70 Oe field in the opposite direction. Figure 2(c) also displays the partially completed hysteresis loops at a number of temperatures. Neglecting the small remnant, the shape of the nonlinear component of the magnetization below T_N resembles somewhat that of a Brillouin function with varying large moment.

The strongly nonlinear field dependence of the magnetization persists (albeit decreasing with increasing T) for temperatures well above T_N. Specifically, the $M(H)$ curve at $T = 175$ K deviates strongly from linear H dependence in the 10 T range. Indeed comparison of the experimental $M(H, T = 175\ \text{K})$ data to a mean field ferromagnetic model with an effective spin (S_{eff}) and a Curie temperature $T_c = 109$ K would require $S_{\text{eff}} > 3$ to replicate the curvature of the experimental data (see figure 2(b)). Thus the $T = 175$ K nonlinearity of the high field magnetization is clearly inconsistent with the $\sim$1.4 μ_B ($S \sim 0.8$) ferromagnetic component at low temperatures.

3.3. Thermal high field magnetization

To better understand the behaviour exhibited in figure 2, we display magnetization versus temperature plots, at a fixed field, in figure 3(a). To first order, for $H \leqslant 1$ T, an order-parameter-reminiscent shape of the $M(T)$ curves is seen, as in figure 1. It should be noted

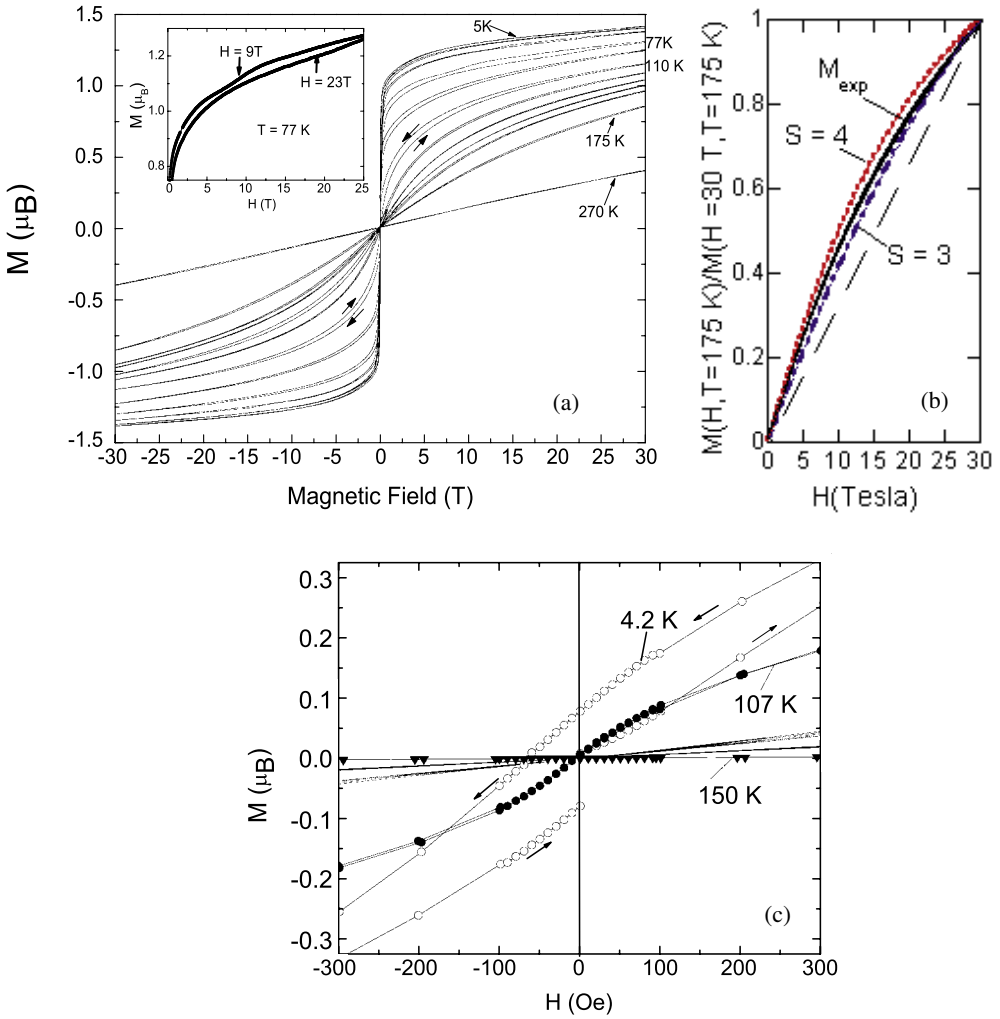

Figure 2. (a) Magnetization (Bohr magneton per Mn ion) versus magnetic field swept up and swept down to 30 T at different temperatures: from the top $T = 5, 30, 50, 77, 100, 110, 120, 130, 140, 150, 175, 270$ K. (b) The magnetic phase transition is clearly evident. The experimental magnetization, $M_{\rm exp}$, (normalized to its value at 30 T) at $T = 175$ K versus magnetic field. Also shown for comparison are the mean-field results calculated for a simple FM material with $T_{\rm c} = 109$ K, with spin $S = 3$ and 4. (c) We display the partially completed hysteresis at low fields loops at a number of temperatures.

that the saturation values of $M(T = 5\ {\rm K}, H)$ increase substantially with increasing H. For $H \geqslant 5$ T the vestiges of the order-parameter dependence persist for $T < T_{\rm N}$, however it 'rides' on a strongly increasing magnetization in the $T > T_{\rm N}$ range. A break in the $M(T, H)$ curves near $T_{\rm N} \sim 105$–110 K also appears to persist up to 30 T, suggesting that the ordering onset is surprisingly field insensitive for a material with a strong AF component. Additionally the very substantial field response, for $H \geqslant 5$ T, appearing at temperatures far above $T_{\rm N}$, is inconsistent with simple AF order. In a FM material, H is thermodynamically conjugate to the order parameter (the DC magnetization), and accordingly a large field response is induced well above the ordering temperature. Since the susceptibility of our $x = 0.875$ material is

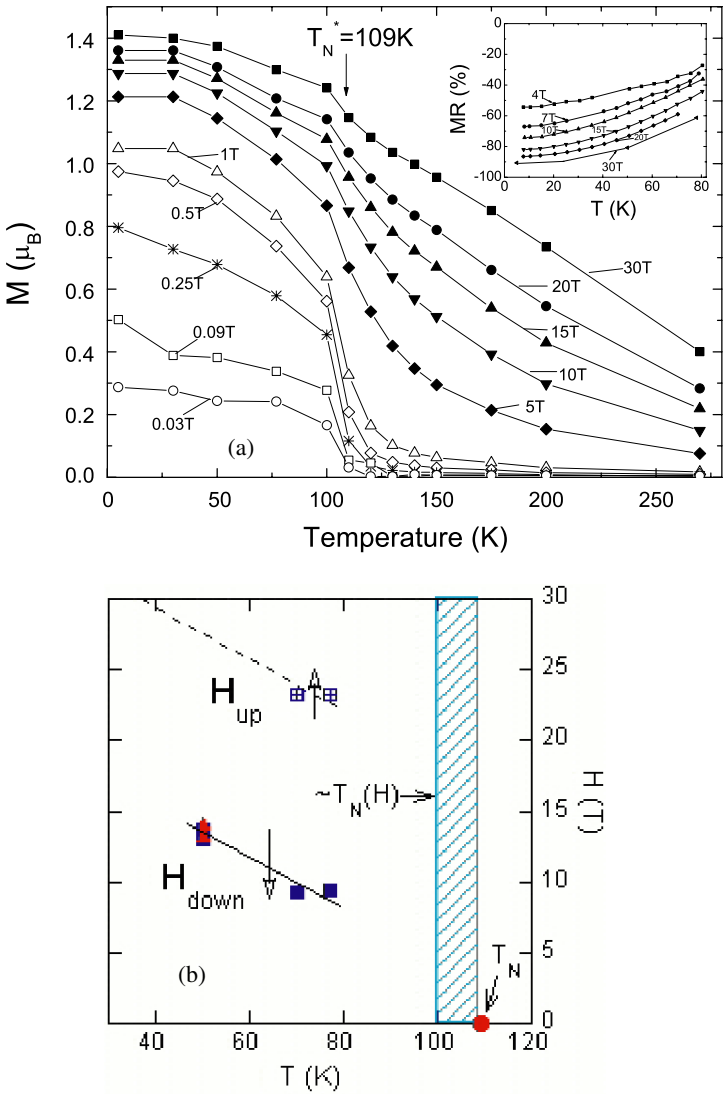

Figure 3. (a) Temperature dependence of the magnetization induced by magnetic fields up to 30 T. Note that the magnetic transition occurs at $T = 106$ K. The inset displays the magnetoresistance (MR). The magnetoresistance at $H = 4$ T is 55% but at $H = 30$ T it is about 90%. (b) The locus in the H–T plane of the magnetization steps $H_{\rm up}$ and $H_{\rm down}$ for a number of experiments. An estimate of the ordering temperature in field $T_{\rm N}(H)$ from the magnetization versus temperature curves (see (a)) is shaded. The $T_{\rm N}$ in zero field is also indicated.

ferromagnetic-like, this large higher-T response is not unexpected, despite the AF component in the ground state. We will return to this point later in the text.

The inset in figure 3(a) displays the magnetoresistance (MR), defined as MR $= (\rho_H - \rho_0)/\rho_0$, where ρ_H and ρ_0 are the resistivities at fields H and zero, respectively. The MR is increasingly negative below $T_{\rm N} = 109$ K. The MR at $H = 4$ T and at $H = 30$ T were found to be approximately -55% and -90%, respectively.

We focus again on figure 2(a), in the region $0 < H < 30$ T. The 77 K magnetization cycle shows small but reproducible nonlinearities for increasing (decreasing) field near $H_{\rm up} = 23$ T

($H_{down} = 9$ T). The 50 K magnetization cycle shows a similar reproducible nonlinearity upon decreasing field near $H_{down} = 14$ T. In figure 3(b) we show the locus of these field nonlinearities from several sets of data, as well as the locus of $T_N(H)$ determined from figures 2(a) and 1. Presumably the H_{up} and H_{down} transitions represent a first order spin flop type transition for those domains where the AF polarization is nearly aligned with the external field. Using the H_{down} versus temperature results to estimate the slope of the metastability limits for this transition, one sees that it should only appear in our magnetization curves between 30 and 80 T. The small size of the nonlinearity in the $T = 50$ K curve presumably is related to the partial completion of the transition in some domains, because the field is 30 T at or below the centre of the H_{up} transition.

3.4. High field magnetization–magnetoresistance correlation

The correlation between the field dependence of the magnetization and the resistivity (at temperatures below T_N) is further explored in figure 4. Note that, as T decreases below T_N, the maximum magnetization does not vary significantly, while the zero field resistivity and magnetoresistance increase enormously. Also, while the magnetization is nearly saturated at 2 T, the resistivity manifests large changes out to 15–20 T. The low field ($H < 1.5$ T) magnetoresistance does exhibit a proportionality to the magnetization squared typical of intergrain tunnelling in ferromagnetic materials [16, 17]. However, the rather large but continuous decrease of the resistivity occurring over a wide range of fields (up to 30 T) would indicate that an additional field induces delocalization of the carriers.

To clarify the magnetoresistance of this material we show the resistivity in fields up to 30 T as a function of temperature (for $T < T_N$) in figure 5. At $H = 0$ the resistivity (magnitude) appears similar to a doped semiconductor with some localization operative for the doped electrons. The absence of a $T \rightarrow 0$ K divergence in the resistivity indicates some itinerant (albeit strongly scattered) electronic states. The largest field effect is the dramatic reduction in the low temperature resistivity rise. This effect would be consistent with a field-induced reduction in the degree of doped electron localization (a reduction in scattering). If one views the localization as electrons retarded (but not trapped) by local potentials, then the field effect could be seen as lowering the depth of these potentials and extending the spatial range of the electronic states. Greater electron hopping and a lower resistivity would result from such a mechanism.

In the inset of figure 5, small but reproducible structures in the resistivity curves near the AF ordering temperature, at 0 and 4 T, are shown. The downturn in the resistivity upon entering the AF state is reminiscent of the critical resistivity anomalies at the AF ordering temperature caused by the loss of spin disorder scattering. The small size of this effect is consistent with the probable dominance of localization over spin disorder scattering in these materials. The field degradation of this anomaly could be consistent with a field induced suppression of spin scattering above the ordering temperature.

3.5. AC susceptibility and time dependent magnetization

The history/time dependence of the magnetization (e.g. see the FC and ZFC magnetization curves in figure 1) is often invoked as evidence for magnetic-glass behaviour such as spin-glass, cluster glass or mictomagnetism. While very similar behaviour is typical of what some authors have referred to as a cluster glass [9, 11, 18–25], this issue is clearly still an open one. (For comparison see a recent example of cluster glass behaviour: the Co based perovskites $La_{0.5}Sr_{0.5}CoO_3$ [11, 19, 23, 24].) To experimentally address the potential glassy character

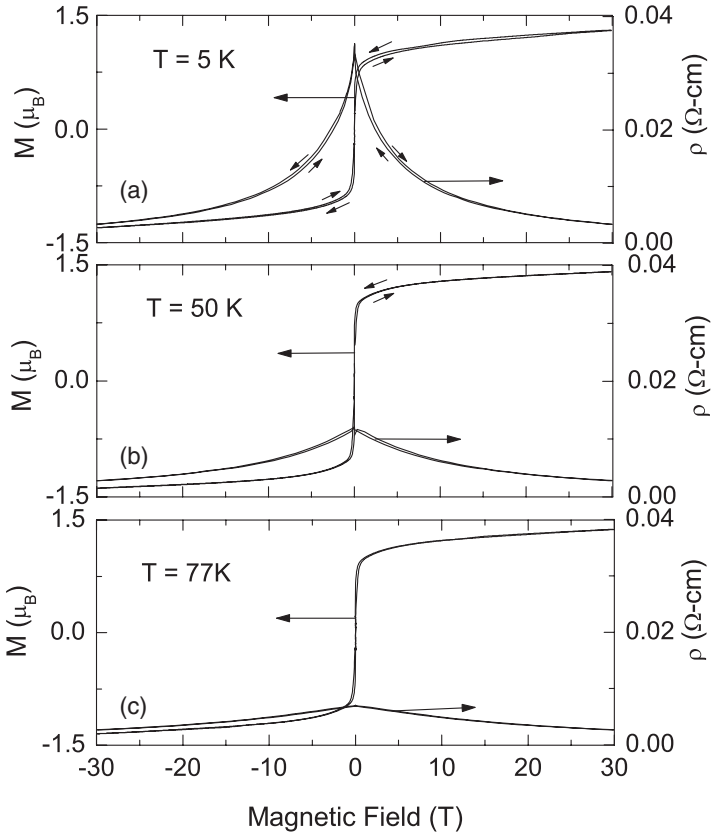

Figure 4. Magnetization (Bohr magneton per Mn ion) and resistivity correlations in applied fields tracing the path: 0 T → 30 T → 0 T → −30 T → 0 T. The curves are for 5, 50 and 77 K in (a), (b) and (c), respectively. Note that while the magnetization is constant, the resistivity is reduced with increasing temperature.

in our $x = 0.875$ BCMO material, we have measured both the frequency dependent AC susceptibility (see figures 6(a) and (b)), and the time evolution of the ZFC moments (see figure 7). As we will see, our AC-χ results indicate a strong coupling of the magnetization to the AF order parameter. Whether this coupling arises through AF spin canting or a more sophisticated ferromagnetic cluster coupling is not clear. The results also show time dependent and dissipative behaviour which could be related to canted-AF-domain and/or glassy effects. In our discussion we will lean toward a canted-AF-domain interpretation.

The AC susceptibility is expressed as $\chi_{ac}(\omega, T) = \chi'(\omega, T) - i\chi''(\omega, T)$, where χ' is the in-phase and χ'' the out-of-phase susceptibility components [26]. The in-phase χ' term is the frequency dependent extension of the DC susceptibility in figure 1 (except that + to − swings in the field are used). The out-of-phase χ'' term is a measure of the magnetic energy dissipation in the sample and is often associated with the degree of hysteresis loop energy absorption.

The connection of χ' to the $\omega = 0$ DC results is manifested in a number of ways. In the plot of χ'^{-1} versus T, shown in figure 6(a) (inset), the FM-like CW high temperature behaviour is clear in precise analogy to the DC-χ^{-1} behaviour in figure 1. Indeed even the details of the estimated ordering temperature of 109 K, and the downward departure of the data, just above T_N, are faithfully replicated in the AC-χ'^{-1} and DC-χ^{-1} behaviour. There is also a

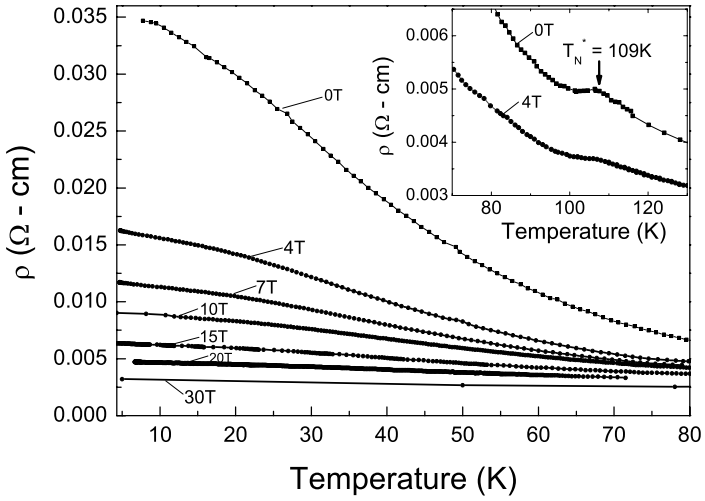

Figure 5. Electrical resistivity versus temperature at fixed field. The magnitude of resistivity near 30 T indicates semiconductor-type behaviour. The inset shows the anomaly at 109 K at 0 and 4 T with tiny shoulder. Note that a broad range of measurements performed on different experimental systems resulted in an uncertainty of 3 K in the determination of the transition temperature.

qualitative similarity in structure between the below-T_N χ' results in figure 6 and the DC-ZFC magnetization curve in figure 1: in both, one observes a negative inflection at 109 K, a peak within 5° below T_N, and a change from sharp concave to slowly varying convex curvature between 10–15 K below T_N. The strongly nonlinear increase in magnetic response, with field (seen in all of the DC results), is also evident even in these low AC-fields. Specifically, comparing the vertical scales in figures 6(a) and (b) one finds that χ' (10 Oe) is nearly five-fold larger than χ' (0.1 Oe). The modest decreases in χ' at higher frequencies is appreciable only in the 50 K $< T <$ T_N range, where the dissipation (χ'') is also large. Finally it is worth noting that the magnitude of χ' at low temperatures reaches (and remains near) a maximum near 20 K. This would suggest that there appear to be a population of spins/spin-clusters that are free enough to respond to small fields far below T_N.

The behaviour of χ'' is related to the dependence of the magnetic energy dissipation in the ordered phase. Figure 6(b) (inset) compares the detailed temperature dependence of χ' and χ'' near T_N. The nonlinear onset of χ'' is displaced slightly lower in temperature relative to the χ' onset. Moreover, the sharp peak in the dissipation appears to coincide with the positive inflection point on the low-T side of the χ' peak. This relation is consistent with the growth of ordered canted-AF domains (and therefore the domain net moments) below T_N. The downturn in χ' reflects the AF locking of some of the spins and the peaking of χ'' reflects the concomitant onset of hysteresis loop energy dissipation. Here the field coupling to the AF domain is through its net uncompensated moment. As T is further lowered, the order parameter and coercive field for domains increase to far above the AC-field. This leads to the low-T quenching of χ'' as the domain reorientation dissipating freezes out. Similarly comparing the χ'' (0.1 Oe) and χ'' (10 Oe) results one notes a 10–15 fold increase in magnitude which extends over a much wider temperature range in the higher field case. This would be consistent with the large field-induced enhancement of the magnetic response, and with it the ensemble of domains active in hysteresis-loop energy dissipation.

The strong frequency/temperature dependence of χ'' (relative to χ') can also be discussed in terms of the domain effects. Specifically the smaller clusters/domains will have a more rapid

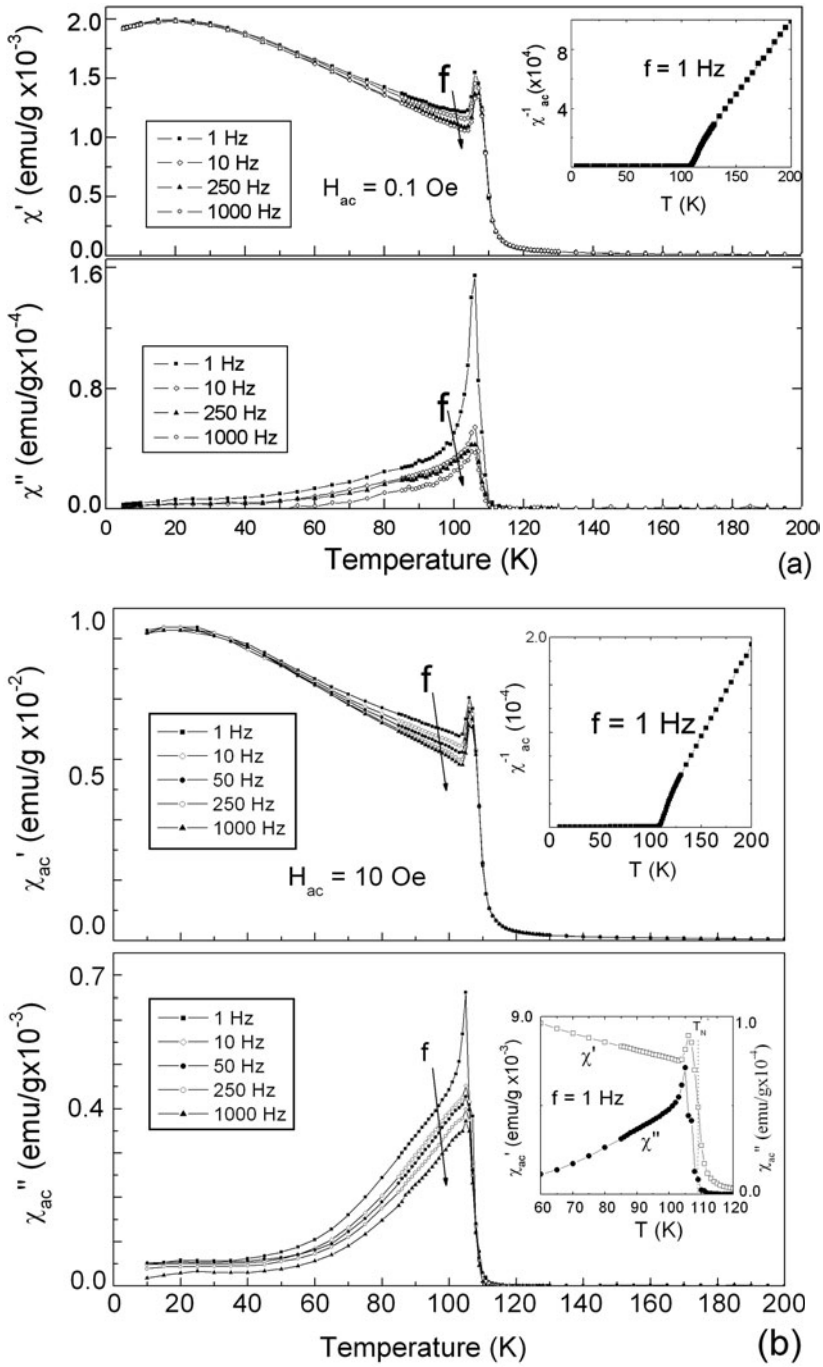

Figure 6. The temperature dependence of the real part χ' and imaginary part χ'' of the ZFC. AC magnetic susceptibilities in varying frequencies, 1, 10, 250 and 1000 Hz for $H = 0.1$ Oe (a), and 1, 10, 50, 250 and 1000 Hz for $H = 10$ Oe (b). The insets show the inverse susceptibility which compares well with the DC results of figure 1. The lower inset of (b) compares the detailed temperature dependence of χ' and χ'' near T_N. The nonlinear onset of χ'' is displaced slightly lower in temperatures relative to the χ' onset.

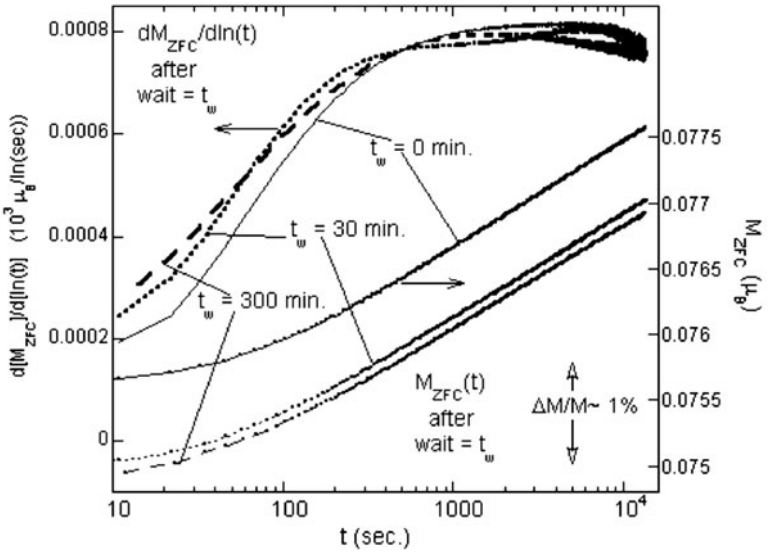

Figure 7. The temporal evolution (logarithmic scale) of the magnetization, and its relaxation rate $\{dM_{ZFC}/d\ln(t)$ versus $\log(t)\}$ for three different 'waiting times' $t_w = 0$, 30 and 300 min. This measurement entailed: cooling the material in zero field to $T = 20$ K; allowing a 'waiting time' to transpire; raising the field to $H = 20$ Oe; measuring the temporal evolution of the magnetization.

response time whereas the larger domains will respond more ponderously. Thus the higher frequency degradation of χ'' should follow the loss of the number domains able to respond at shorter response times. The precipitous decay of the χ'' ($H = 0.1$ Oe, $f = 1$ Hz) below its peak perhaps best illustrates both the rapid freezing out of available domains with low-coercive fields and short response times. These detailed correlations should be incorporated into a proper theory of the AF-domain, and of cluster and glass-like effects in this material; however, such a model is not clear at this time.

Certainly some of the AC susceptibility features exhibited here are similar to those exhibited in CG systems; however, there are also disparities. Indeed, it should be noted that there are also substantial disparities (in AC susceptibility behaviour) between different so called 'cluster glass' systems [23, 25]. Thus portions of the AC susceptibility would appear to fit into the somewhat broadly defined cluster glass category. The presence of a strong underlying AF order would appear to set this system apart from other CG systems.

An additional measurement to probe for magnetic glassy behaviour is the slow long term response of the system to an applied magnetic field. In figure 7 (bottom) we show the evolution of the ZFC magnetization for wait times $t_w = 0$, 30 and 300 min. The measurements were performed by cooling in zero field, waiting for time, t_w, before applying a 20 Oe magnetic field, and then recording the magnetization as a function of time.

The magnitude of these glassy effects can be seen from the figure to be modest (i.e. a few per cent). The magnitudes of the magnetization are also uniformly smaller for longer wait times after the temperature 'quench'. This indicates a slow relaxation (upon cooling) into a more magnetically frustrated state, which is less responsive to external field. The magnitude of the time dependent magnetization as a function of waiting time is similar to that observed in the $La_{0.5}Sr_{0.5}CoO_3$ CG system [23].

The logarithmic time evolution of the magnetization appears to support a distribution of timescales in the relaxation. The logarithmic time derivative or the ZFC magnetization

evolution is shown in figure 7 (upper curves). These derivative curves do not show a characteristic maximum occurring at the wait time, as seen in the SG $La_{0.91}Sr_{0.09}CoO_3$ [11].

Thus the time/frequency dependent magnetic behaviour of the $x = 0.875$ BCMO material does exhibit glassy effects in addition to cluster effects. The observed trends are broadly consistent with cluster glass behaviour [11, 27] with the broadness and somewhat imprecise definition of such behaviour being recognized.

3.6. Clustering considerations

Several points are worth noting regarding the magnetic properties of electron-doped manganites like the $Bi_{1-x}Ca_xMnO_3$ $x = 0.875$ material studied in this paper. G-type AF order in $CaMnO_3$ has been shown to persist in these materials with doping up to levels similar to our $x = 0.875$ material. Indeed the AF ordering temperature in these electron-doped materials is changed little from that found in the undoped parent compound (i.e. T_N is in the 109–120 K range). Although a substantial net moment does appear at low fields in these materials, the onset of this moment is closely coincident with the AF ordering temperature (as opposed to higher or lower). Thus G-type AF interactions with an energy scale $\sim T_N$ would appear to be a fundamental component in understanding the magnetic properties of these materials.

The saturation of the resistivity at a finite (though large) low temperature limit would suggest a population of partially electron itinerant-doped electrons. The coexistence of electron hopping and AF order are the key ingredients for the DeGenes model of canted antiferromagnetism in these types of materials [28]. One must therefore carefully consider the canted AF explanations for this material's behaviour. Certainly local deviations from a homogeneous canted AF state would be present; however, the occurrence of a distinct glassy state is an open question.

In our discussion of figure 1 we noted the similarity of the field-cooled magnetization, $M_{FC}(T)$, to a temperature dependence on the order parameter below a magnetic transition. We have critically compared the rise in the magnetization below T_N in figure 1, to the critical behaviour $(1 - T/T_N)^{\beta}$, with the mean field $\beta = 1/2$, and with $\beta = 1/3$ which is closer to the experimental measurement of $\beta = 0.368(0.01)$ for a similar electron-doped material [5]. The $M_{FC}(T)$ is found to rise and saturate more quickly than either of these. Including nonlinear effects in the mean field case, by iteratively solving the Brillouin function for the spontaneous field, steepens the temperature dependence toward the experimental data but not sufficiently. Nonlinear effects within a non-mean field $\beta = 1/3$ model should improve still more the notion of a coupling (to first order only) of the low field moment $M_{FC}(T)$ to the order parameter. However, the full, detailed dependence of $M_{FC}(T)$ on the order parameter (as well as T and H) is certainly much more complex than linear.

This notion would suggest a first order coupling of the low field magnetization (or the effective magnetic moment u_{eff}) to the order parameter for a G-type AF, the staggered magnetization ($M_S = M_A - M_B$, where the A and B refer to the AF sub-lattices). Recall also that we noted, for temperatures well above T_N, the magnetic susceptibility can be fit to a CW-type susceptibility $\chi = C/(T + \theta)$ with θ close to $-T_N$ (rather than the $+T_N$ value expected for a G-type AF). The below T_N behaviour could result from the canted-moment component coupled to the AF order. It should be noted that the FM clusters within the AF domain were proposed by Neumeier *et al*. An explanation in terms of phase segregated FM regions would appear more demanding. At this juncture we will consider extending the notion of a first order linear coupling between M_S and u_{eff} to $T > T_N$ purely phenomenologically.

Above T_N there is no average sublattice magnetization and no static AF domains. However, there are temporal and spatial AF fluctuations. As T approaches T_N from above, the AF

fluctuation divergence is governed by the staggered susceptibility $\chi_S \sim (T - T_N)^{-\gamma}$ (with $\gamma = 1$ for the mean field value assumed here). Within our first order coupling assumption, the magnitude of the magnetization should track this divergence, qualitatively explaining the $\chi \sim (T - T_N)$ behaviour observed.

To be more quantitative, after Landau and Lifshitz [29] and directly from the fluctuation dissipation theorem, the mean squared order parameter fluctuations above T_N go like $\bar{M_S} = 0$, one should have

$$\langle(\delta M_S)^2\rangle \sim \chi_S, \tag{1}$$

since in this high T range

$$\langle(M_S)^2\rangle \sim \chi_S \sim [T - T_N]^{-1}.$$

Invoking the ordered state behaviour, a given AF fluctuation/domain would have an uncompensated effective DC magnetic moment (u_{eff}), with the bigger the M_S, the bigger the moment. Specifically, the u_{eff} of such an AF fluctuation, should be coupled linearly to the local staggered magnetization. Thus one would expect the average susceptibility of an ensemble of such moments, each associated with an AF fluctuation, to have a Curie susceptibility,

$$\chi_c = \frac{C_{eff}}{T}$$

where $C_{eff} \sim \mu_{eff}^2$, but with a temperature dependent Curie constant given approximately by

$$C_{eff} \sim \mu_{eff}^2 \sim \langle(M_S)^2\rangle \sim \chi_S \sim [T - T_N]^{-1}.$$

Therefore the explicit T-dependence of this contribution to the susceptibility should approximately be

$$\chi_c = \frac{C_2}{T}\frac{1}{[T - T_N]}.$$

The overall susceptibility should also contain a term due to the AF interacting spins (not involved in the uncompensated moments) yielding an overall susceptibility

$$\chi = \frac{C_1}{[T + T_N]} + \frac{C_2}{T[T - T_N]}.$$

Given a sufficient number of uncompensated moments, the susceptibility is dominated by the second diverging term, thereby yielding CW behaviour with the 'wrong' sign for the Weiss temperature for an AF.

To illustrate the viability of the above notion we show, in figure 8(a), the experimental inverse susceptibility, along with the predictions of our model. $T_N = 109$ K was fixed and the C_1 and C_2 were adjusted to track the data. The model–experimental agreement is quite encouraging despite the simplicity of the model. Note that for χ^{-1} the model correctly replicates the high temperature FM-like CW parameter and the downward curvature away from CW behaviour as T approaches T_N from above (see figures 1 and 6(a) (inset)).

Using the value of C_2 one can estimate the temperature dependence of the effective cluster spin (per doped electron), as shown in figure 8(b). The notion of the existence of an effective cluster moment (in each AF fluctuation) is also supported by the strongly nonlinear field dependence of the magnetization at 175 K (65 K above the ordering temperature) noted in the discussion of figure 2(a).

Turning to the below T_N behaviour, we note that the strongly nonlinear high field magnetization curves (neglecting the very small remnant) are in fact reminiscent of superparamagnetism exhibited by large collectives of moments acting as clusters (see figures 2(a) and (b)). To illustrate this we first estimate the linear field response from the

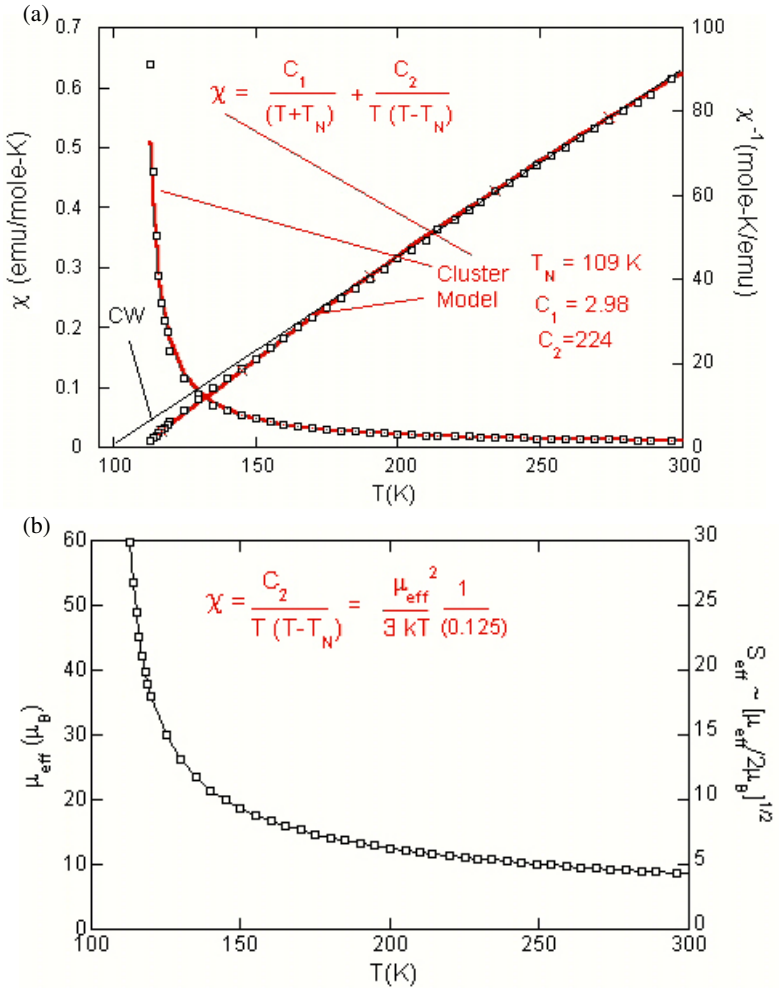

Figure 8. (a) The experimental magnetic susceptibility (χ) and its inverse (χ^{-1}) plotted as open squares. The heavy solid curves are the model (formula shown in the figure). $T_N = 109$ K was fixed in accordance with the observed ordering temperature. The C_1 and C_2 parameters were adjusted to follow the data. The high temperature CW [$\chi = C/(T + \theta)$] fit to the data yields $\theta = 99.6$ K and $C = 2.23$ emu mol^{-1} K^{-1} (or $\mu_{\rm eff} = 4.23\ \mu_{\rm B}$). (b) The value of $\mu_{\rm eff}$ (per doped electron) and $S_{\rm eff}$ in the cluster term from (a). Note $\mu_{\rm eff}^2 = g^2 S_{\rm eff}(S_{\rm eff} + 1) \sim g^2 S_{\rm eff}^2$ has been used.

highest field slope of the low temperature magnetization data. After subtraction of this linear term, our experimental magnetization curve at 65 K was normalized to its value at 30 T and plotted versus H/T in figure 9. For comparison, plots of the Brillouin function versus H/T for differing spin values are also shown in figure 9. Clearly the field dependence must be more complicated. However, based on the saturation-shoulder in this comparison, the experimental results would appear to be consistent with an effective uncompensated spin clusters with S of the order of ∼200.

Within the canted AF interpretation these moments would be associated with single AF domains, each with its own canting direction. The zero-field randomly oriented domains would become aligned with the canting direction along a sufficiently large external field. The magnitude of the canting component of the spin would also be expected to be enhanced in

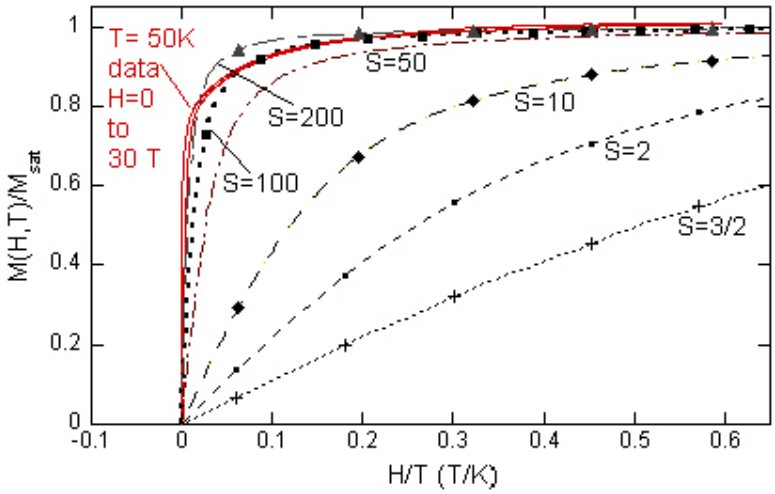

Figure 9. The linear-corrected and normalized experimental magnetization (solid curve) at $T = 50$ K and $0 \leqslant H \leqslant 30$ T, plotted versus H/T. The linear correction involves subtracting a linear-background term, determined from the high field slope, from the experimental data, $M_{\rm exp}$[i.e. $M(H, T = 50\ {\rm K}) = M_{\rm exp} - H(0.0052\ \mu_{\rm B}\ {\rm T}^{-1})$]. The corrected magnetization is then divided by its saturation value at $H = 30$ T (1.21 $\mu_{\rm B}$ in this case) for comparison to the Brillouin function $B_{\rm S}(H/T)$ with differing spin values S. The Brillouin function plots are all non-solid lines to differentiate them from the experimental results.

field; upon decreasing the field the domains would have to de-align to produce the low remnant magnetization.

Thus above and below $T_{\rm N}$ the magnetic response would appear to be consistent with the respective presence of AF fluctuations and domains with large net moments. This consistency follows from the first order coupling of the DC magnetization to the AF order parameter (the staggered magnetization). It should be noted that such a relationship, $M \alpha M_{\rm S}$, coupling is explicitly present in the theory of canted antiferromagnetism [28].

4. Discussion and overview

The observed magnetoresistance of this material supports a field-induced enhanced demoralization of the doped electrons in this system. The notion that the doped electrons in such materials induce local-FM double exchange interactions in such materials has been generally assumed in the past. Recently neutron scattering on these materials has also confirmed the fundamental importance of a G-type AF order in the ground state of these materials [30]. The incorporation of these ideas into FM-like effects in these electron-doped materials has typically involved invoking a FM-spin canting accompanying the AF order, or a phase segregation (on some scale) in which electron rich regions could be ferromagnetic with an electron poor AF background.

The FM segregation has a potential problem with the absence of any nearby truly metallic FM phase and the apparent requirement that doped electrons should segregate at an appreciable distance from the Bi site to which they owe their charge neutrality. Our results also present another plausible Ocums-razor challenge to this notion. Specifically the FM interactions at high temperature are reflected in the negative Weiss constant in the susceptibility $\theta = -100$ K which is extremely close to the G-type AF ordering at $T_{\rm N} \sim 109$ K. If the FM effects are

related to segregated regions, why should their energy scale be so similar (as opposed to much larger/smaller) compared to the AF scale. On the other hand our proposal and more traditional treatments of spin canting axiomatically involve a linear coupling between the AF and FM order parameters and their apparent onset temperatures. Indeed the detailed curvature of the inverse susceptibility close to T_N is consistent with the canted AF interpretation. Thus while both the canted AF and segregated FM interpretations must both still be considered viable we would favour the former.

Our results do show time/history effects associated with cluster glass systems. Frustrated and non-equilibrium interactions between canted AF domains may be a source of these glass-like effects. Along these lines the concept of a cluster glass would appear to need some clarification before this system could be clearly placed in this category.

The authors would like to propose a test of the FM phase segregation versus canted AF interpretations of the magnetism in this system. For the canted AF, there is a linear coupling between the DC magnetization and the staggered magnetization at temperatures both below and above the ordering temperature. Thus an external H field (above T_N) which induces a DC magnetization should also induce a staggered (AF) order parameter. Such field induced AF correlations (above T_N) may be detectable as magnetic Bragg peaks in neutron scattering. For the case of the segregated FM the external field should stabilize FM regions and while making AF correlations still more unfavourable. High field neutron scattering measurements may therefore provide some insight into this problem.

5. Conclusions

Detailed magnetic and transport measurements of the electron doped $Bi_{0.125}Ca_{0.875}MnO_3$ materials have been performed. Low field magnetization measurements evidence ferromagnetic Curie–Weiss behaviour at higher temperatures and an antiferromagnetic state below $T_N = 109$ K which supports a ferromagnetic component. High field ($-30\ \text{T} \leqslant H \leqslant 30\ \text{T}$) DC magnetization measurements (5–300 K) show strongly nonlinear field responses below and far above the ordering temperature. The residual magnetic moment and coercive field, in the ordered state, are, however, exceptionally small. The glassy character of the cluster magnetic response was investigated by measuring the frequency dependent AC susceptibility and time/history evolution of the low field magnetization. Glassy behaviour in the cluster response is indeed observed. The differentiation of cluster glass versus canted AF origins of the time/history effects is still an open issue to be addressed in future work.

Acknowledgments

We thank Dr M Uehara of the Rutgers University Physics Department for assistance in sample preparation that was funded by the NSF-DMR-9802513 (S-W Cheong). We also thank Dr A Millis, Dr J M Tranquada, Dr S Shapiro and G Shirane for valuable discussions and Dr Y Gulak for valuable help with numerical modelling. We are indebted to Mr Guerman Popov for assistance in DC magnetization measurements at the Department of Chemistry, Rutgers University. The authors thank Mr S Baily and Dr M Salaman at the Department of Physics, University of Illinois at Urbana-Champaign, for useful discussion and AC susceptibility measurements. Magnetic measurements in high fields up to 30 T were performed at the National High Magnetic Field Laboratory, which is supported by NSF Cooperative Agreement No DMR-9527035 and by the State of Florida. We are grateful to Dr Bruce L Brandt, Dr Scott T Hannahs and Dr M Whitton for assisting with resistivity measurements, and Dr D Hall for

assisting with the VSM. This research was funded by DOE Grant DE-FG02-97ER45665 and the New Jersey Space Grant Consortium (NASA).

References

[1a] Jonker G H and Van Santen J H 1950 *Physica* **16** 337
[1b] Macchesney J B, Williams H J, Potter J F and Sherwood R C 1967 *Phys. Rev.* **164** 779
[1c] Ramirez A P 1997 *J. Phys.: Condens. Matter* **9** 8171
[1d] Rao C N R and Raveau B 1998 *Colossal Magnetoresistance, Charge Ordering Related Properties of Manganese Oxides* (Singapore: World Scientific)
[1e] Tokura Y and Tomioka Y 1999 *J. Magn. Magn. Mater.* **200** 1
[1f] Coey J M D, Viret M and von Molnar S 1999 *Adv. Phys.* **48** 167
[1g] Cheong S-W and Hwang H Y 2000 *Colossal Magnetoresistive Oxides* ed Y Tokura (New York: Gordon and Breach)
[1h] Uehera M, Kim K H and Cheong S-W (a rich phase diagram for LCMO) unpublished
[1i] Rao C N R, Arulraj A, Cheetham A K and Raveau B 2000 *J. Phys.: Condens. Matter* **12** R83
[2] Wollan E O and Koehler W C 1955 *Phys. Rev.* **100** 545
Goodenough J B 1955 *Phys. Rev.* **100** 564
[3] Moreo A, Yunoki S and Dagotto E 1999 *Science* **283** 2034
[4] Neumeier J J and Cohn J L 2000 *Phys. Rev.* B **61** 14319
[5] Hagdorn K, Hohlwein D, Ihringer J, Knorr K, Prandl W, Ritter H, Schmid H and Zeiske Th 1999 *Eur. Phys. J.* B **11** 243
[6] Schiffer P, Ramirez A P, Bao W and Cheong S-W 1995 *Phys. Rev. Lett.* **75** 3336
Ramirez A P, Cheong S-W and Schiffer P 1997 *J. Appl. Phys.* **81** 5337
[7] Woo H, Tyson T A, Croft M, Cheong S-W and Woicik J C 2001 *Phys. Rev.* B **63** 134412
[8] Chiba H, Kikuchi M, Kusuba K, Muraoka Y and Syono Y 1996 *Solid State Commun.* **99** 499
[9] Maignan A, Martin C, Damay F, Raveau B and Hejtmanek J 1998 *Phys. Rev.* B **58** 2758
[10] Martin C, Maignan A, Hervieu M and Raveau B 1999 *Phys. Rev.* B **60** 12191
[11] Itoh M, Natori I, Kubota S and Motya K 1994 *J. Phys. Soc. Japan* **63** 1486
[12] Troyanchuk I O, Samsonenko N V, Szymczak H and Nabialek A 1997 *J. Solid State Chem.* **131** 144
[13] Hwang H Y, Cheong S-W, Radaelli P G, Marezio M and Batlogg B 1995 *Phys. Rev. Lett.* **75** 914
[14] Taguchi H 1985 *Phys. Status Solidi* a **88** K79
[15] Bao W, Axe J D, Chen C H and Cheong S-W 1997 *Phys. Rev. Lett.* **78** 543
[16] Hwang H Y, Cheong S-W, Ong N P and Batlogg B 1996 *Phys. Rev. Lett.* **77** 2041
[17] Zeng Z, Greenblatt M, Subramanian M A and Croft M 1999 *Phys. Rev. Lett.* **82** 3164
[18] Koyano M, Suezawa M, Watanabe H and Inoue M 1994 *J. Phys. Soc. Japan* **63** 1114
[19] Mukherjee S, Ranganathan R, Anilkumar R S and Joy P A 1996 *Phys. Rev.* B **54** 9267
[20] Gayathri N, Raychaudhuri A K, Tiwary S K, Gundakaram R, Arulraj A and Rao C N R 1997 *Phys. Rev.* B **56** 1345
[21] Maignan A, Martin C, Damay F and Raveau B 1997 *Z. Phys.* B **104** 21
[22] Negishi H, Ohara S, Koyano M, Inoue M, Sakakibara T and Goto T 1988 *J. Phys. Soc. Japan* **57** 4083
[23] Nam D N H, Jonason K, Nordblad P, Khiem N V and Phuc N X 1999 *Phys. Rev.* B **59** 4189
[24] Kumar P S A, Joy P A and Date S K 1998 *J. Phys.: Condens. Matter* **10** L487
[25] Pejakovic D A, Manson J L, Miller J S and Epstein A J 2000 *J. Appl. Phys.* **87** 6028
[26] Mydosh J A 1993 *Spin Glasses: an Experimental Introduction* (London: Taylor and Francis)
[27] Pejaković D A, Manson J L, Miller J S and Epstein A J 2000 *Phys. Rev. Lett.* **85** 1994
[28] de Gennes P-G 1960 *Phys. Rev.* **118** 141
Matsuura M, Ajiro Y and Haseda T 1969 *J. Phys. Soc. Japan* **26** 665
[29] Landau L and Lifshitz E 1980 *Statistical Physics* part 1, 3rd edn (New York: Pergamon) p 472 and additional references within that work mentioned on this page (reprinted 1982)
[30] Santhosh P N, Goldberger J, Woodward P M, Vogt T, Lee W P and Epstein A J 2000 *Phys. Rev.* B **62** 14928